Free Space Optical Communication Systems Exploring Advanced Modulation Formats

Rui Miguel Coelho do Carmo
IST-Universidade de Lisboa,
Av. Rovisco Pais, 1049-001 Lisboa
e-mail: rmcarmo@academiafa.edu.pt;

Abstract—**In the near future, one of the solutions for the exponential increase in bandwidth requirements and transmission capacity will be the transition of wireless communications to its fifth generation (5G), which will represent an important step in the fast-paced evolution of telecommunications. In this context, the use of free-space optical links will undoubtedly be a valuable asset for improving the coverage, capacity and overall quality of experience in the datacenters and in urban centers as it is a flexible and low-cost solution. It is possible to propose optical backhaul solutions with high capacity, spectral and energy efficiency, but also with low cost per bit.**

Thus, the present work proposes the study of advanced modulation formats, with potentiality of application in optical communication systems in free-space, favoring the possibility of using direct detection. In this sense, a project will be carried out, consisting on the implementation of a low-cost point-to-point optical communications module, operating in the visible spectral region and based on the direct modulation of the optical emitter. By modulating a subcarrier, the BPSK and QPSK formats are used, thus allowing increased spectral efficiency of the connection. From QPSK modulation, it was able to achieve an EVM(%) of 1.3%.

Keywords— Free-space optical communications, advanced modulation formats, phase modulation, subcarrier modulation, direct detection.

I. INTRODUCTION

In recent years there has been a great growth and advance in Information and Communication Technologies, which are recognized as responsible for major changes in the development of the global economy. With increasing use of the internet, with ever-higher transmission rate requirements for a variety of applications, such as videoconferencing and live-streaming, it has been clear that bandwidth requirements and transmission capacity are increasing exponentially. One of the consequences of this growing trend is the need to introduce optical technologies into the access network and the congestion of the spectrum used in conventional radiofrequency systems [1], [2].

In the near future, the escalation of this evolution will have another important step: the transition from wireless to its fifth generation (5G). The 5G technology provides for the resolution of six challenges that are not effectively resolved by 4G, namely: increased transport capacity, higher transmission rate, lower end-to-end latency, massive device connectivity, reduced cost and consistent supply of Quality of Experience [3]. In this context, it is important to note that 5G wireless communications do not only cover optical connections or radio communications. It is a technology that encompasses the entire network infrastructure, from the optical network core to the radio access network.

The data transport network from the core to the local access point is only feasible through the exploitation of high capacity optical technologies such as Spatial-Division-Multiplexing, based on advanced modulation techniques and coherent detection. However, the use of free-space links can contribute to the improvement of coverage, capacity and the overall Quality of Experience in datacenters and urban centers, since it is a flexible and low cost solution. This type of solution will prove to be of major importance in meeting the growing demand for bandwidth and challenging demands arising from new applications in high capacity 5G networks [3].

Of the many applications of free-space communication systems (FSO - Free-Space-Optics) are the connections involving satellites, probes, aircraft, ground stations, unmanned aerial vehicles (UAVs), high altitude platforms, among others. In addition, all these connections can be used in both military and civilian contexts, which greatly increases their utility and versatility [1]. Nevertheless, the fact that there are only a few free-space optical links between fixed locations shows that their use has not necessarily been highlighted in terrestrial communications. However, for high transmission rates (>10 Gbit/s) and range of around 3 to 5 km, there is a niche market for FSO systems. In 2008, MRV Communications introduced a system with a transmission rate of 10 Gbit/s, claiming a distance of 2 km in high availability [4]. However, this equipment is no longer available [4]. In 2013 the company MOSTCOM introduced the Artolink M1-10GE, being also able to obtain rates of transmission of 10 Gbit / s and an improved range of 2.5 km. Under laboratory conditions, this company, together with the "Fiord" Scientific and Technological Center, was able to achieve 30 Gbit/s transmission rates [5].

This type of technology requires devices similar to those used in fiber optics, the only difference being the channel in which its transmission is made. This system has some advantages, such as: no need to open ducts to install cables, having a quick and efficient installation; Does not require licenses and permissions; The bandwidth can be higher than or equal to the fiber optic systems and much higher than the RF systems, being able to reach the order of Tbit/s; and do not induce electromagnetic interference with other equipment. On the other hand, its main disadvantage is that it is quite difficult to acquire, to track and to align due to the divergence and size of the beam. In addition, FSO communications are heavily dependent on unpredictable atmospheric conditions, which can degrade system performance. Another limiting factor is also the interference of radiation sources [2]. In this way, it is essential to study and test new techniques and new modulation formats that are increasingly advanced and complex, so that can satisfy this increasing demand for bandwidth and for a higher distance.

In this paper we propose the development and implementation of an optical communications module, operating in the visible spectral region, based on the direct modulation of the optical emitter, with the purpose of being implemented as a low-cost backhaul optical system, where the reliability of its application should be assessed.

This work is organized as follows: after an introduction, the channel characterization and the theory of BPSK, QPSK and EVM implementation is presented in section II. Section III deals with all de hardware and software used. Section IV deals with the implementation of the module with BPSK modulation and a LED as an optical emitter. Section V deals with the implementation of the module with QPSK modulation and a semiconductor laser as an optical emitter, where the EVM will be used to quantify the system performance. Finally, the main conclusions are drawn in section VI.

II. THEORETICAL FUNDATION

In this work, an electric subcarrier was used in order to modulate an optical carrier, generated by the optical emitter, whose detection is based on the direct detection, thus allowing to extract the subcarrier and later to process it numerically.

A. Free-Space Propagation

FSO technologies use the atmospheric channel as a propagation medium whose properties are random functions of space and time, which makes FSO connections a phenomenon dependent on climate and geographic location. Various unpredictable environmental factors, such as clouds, snow, fog, rain, fog and so on, are strong attenuators in the optical signal, limiting the binding distance that can be applied. If the connection is considered to be unaffected by the atmosphere in the basic free-space channel, the signal is transmitted without any loss. Otherwise, if one considers the extinction effects of the atmosphere, it is well known that several factors contribute to the degradation of the received signal. Under good climatic conditions, the losses in the atmospheric channel are mainly due to absorption and dispersion phenomenon [6].

Atmospheric absorption is caused by the interaction between photons and atmospheric molecules along the transmission path, such as ozone, water vapor and CO2. When some of the photons are extinguished, their energy turns into heat. The atmospheric molecular concentration depends on the pressure and temperature that vary with time, altitude and geographic location. Absorption varies depending on the wavelength [7].

Atmospheric dispersion causes angular fluctuations. Optical radiation is dispersed due to molecular particles, which is called the Rayleigh scattering process. When the particle size is large, compared to the transmission wavelength, the process is called the Mie dispersion, which is much less dependent on the wavelength, whereas the Rayleigh scattering is predominant at short wavelengths [7].

The calculation of the attenuations caused by fog most often comes from empirical approaches, because they are more convenient when compared with other types of theoretical approaches that are much more complex and time consuming. The most common empirical model is based on the estimation of the visibility reach. Based on the estimate of this range, with a transmission threshold of 2% over the atmospheric path, the fog attenuation can be estimated by [8]:

$$\alpha(\lambda) \cong \frac{17.35}{V}\left(\frac{\lambda}{550}\right)^{-q} \quad (1)$$

where V is the visibility range in km, λ is the transmission wavelength in nm. γ (λ) is the total attenuation coefficient for fog and q is the fog droplet size distribution coefficient. The parameter q in equation (1) depends on the scope of visibility and is given by the following equation [8]:

$$q = \begin{cases} 1.6, & \text{V} > 50\text{km} \\ 1.3, & 6km < V < 50km \\ 0.16V + 0.34, & 1km < V < 6km \\ V - 0.5, & 0.5km < V < 1km \\ 0, & V < 0.5km \end{cases} \quad (2)$$

B. BPSK Modulation

BPSK modulation is the particular form of phase shift keying, using only two values for the phase, separated by 180°, depending on its bits.

This modulation is the most robust of all PSK modulations, since only by taking the highest level of noise or distortion is it possible to make the demodulator come to an incorrect decision. It is, however, only able to modulate 1 bit/symbol and therefore may not be suitable for applications with high transmission rates [9]. During the modulation process, the carrier phase is modified taking into account the information to be transmitted. This process consists in multiplying the signal to be transmitted, which in this case is the digital signal d(t), by the carrier S(t), obtaining the following modulated wave Sbpsk(t) [10]:

$$S_{bpsk}(\text{t}) = \text{A}\cos(w_0 t + \theta(t)) \quad (2)$$

where θ is 0 or π. Schematically, this process is represented by Figure 1 and the modulated wave takes the form represented in Figure 2:

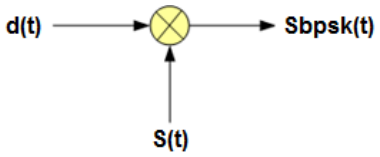

Fig. 1. - BPSK modulation scheme [adapted from [9]]

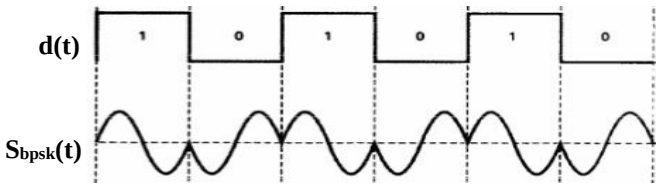

Fig. 2. – Waveform

After sending the signal through the transmission channel, it is necessary to demodulate. The following scheme represents the entire demodulation step:

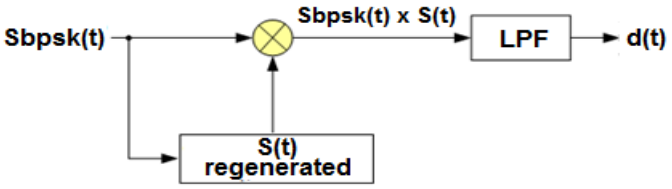

Fig. 3. – BPSK demodulation scheme [adapted from [9]]

First, the received signal is multiplied again by a wave identical to the carrier wave, thus obtaining a signal with twice the frequency of the carrier. This signal is characterized as follows:

$$A_1 A_k \cos(w_0 t) \times \cos(w_0 t + \theta(t)) = \\ = A_1 A_k \frac{1}{2}[\cos(2w_0 t) + \cos(\theta(t))] \quad (4)$$

In this situation, it is expected that when the bit is "1", the modulated component is above zero, while when the bit is "0", the modulated component is below zero. After multiplication, the second step in signal recovery is to apply a low-pass filter (LPF) to the resulting signal in order to remove the oscillatory component at twice the frequency of the carrier, obtaining the following expression:

$$A_1 A_k \frac{1}{2}\cos(\theta(t)) = \begin{cases} \frac{A_1 A_k}{2} \\ -\frac{A_1 A_k}{2} \end{cases} \quad (5)$$

According to the term it is to be expected that the amplitude will decrease by half. Therefore, it is possible to determine the original baseband signal and hence the original bit stream.

Concerning the BPSK constellation diagram (Figure 4), the constellation points lie entirely on the x-axis and therefore have no projection on the y-axis. This means that the BPSK modulated signal will have an in-phase component (I) and no quadrature component (Q).

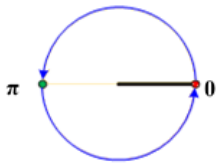

Fig. 4. – BPSK signal constellation

C. QPSK Modulation

As the second and last implementation phase, it is intended to use the QPSK modulation format. The Quadrature Phase Shift Keying modulation allows to transmit the information in four phase transitions (π/4, 3π/4, 5π/4, 7π/4), where each transmitted symbol contains two bits. Thus, these symbols no longer correspond only to "0" or "1", but to {00, 01, 10, 11}, each corresponding to a specific phase transition. This means that the QPSK can be used to double the rate of transmission compared to a BPSK system, maintaining the same signal bandwidth. Or it allows to maintain the same transmission rate of the BPSK, reducing the necessary bandwidth by half [10].

Figure 5 shows the QPSK modulation scheme, where the generated bit sequence is divided into in-phase and quadrature components. These are then modulated separately, as they are multiplied by the carrier in phase (I) Ci (t) and by the quadrature (Q) component Cq (t). Thereafter, the two signals are superimposed and the resulting signal is the QPSK modulated signal. The following equations represent the process:

$$\mathrm{Ci(t)} = \mathrm{A}_k \cos(w_0 t) \quad (6)$$

$$\mathrm{Cq(t)} = \mathrm{B}_k \mathrm{sen}(w_0 t) \quad (7)$$

$$\mathrm{Cq(t)} + \mathrm{Ci(t)} = S_{qpsk}(\mathrm{t}) = \mathrm{A}_k \cos(w_0 t) + \mathrm{B}_k \mathrm{sen}(w_0 t) \quad (8)$$

Note that the polar encoding NRZ can be made before or after the division of the bits. In the case of the figure, they were later placed to illustrate the conceptual difference between digital and analogic signals involved with digital modulation.

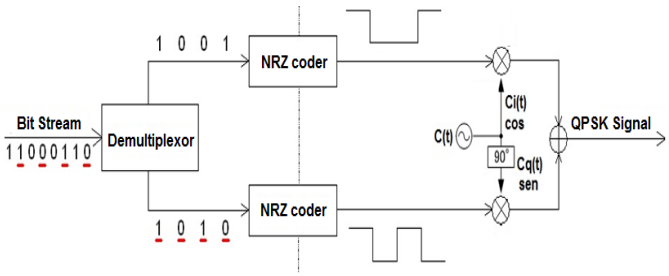

Fig. 5. – QPSK transmitter [adapted from [11]]

After sending the signal through the transmission channel, the demodulation is performed, whose process is shown in Figure 6. First, the received signal is divided into two parts, each of which is multiplied again by a wave similar to Carrier wave in phase and quadrature. Then both components are filtered by an LPF in order to remove the oscillatory component at twice the frequency of the carrier. Each decoding device uses a reference threshold value to determine whether a "1" or "0" is detected. Finally, the two bit sequences are overlapped, forming the original bit sequence.

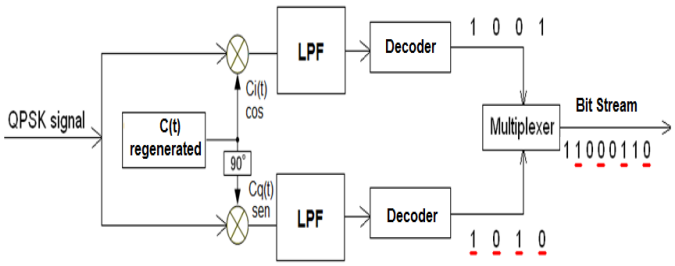

Fig. 6. – QPSK receiver [adapted from [12]]

For the QPSK constellation diagram, the constellation points lie on the two axes of the diagram, using four equidistant points. As shown in Figure 7, the information is assigned to the carrier wave phases π/4, 3π/4, -π/4 and -3π/4 as respectively 00, 01, 10 and 11.

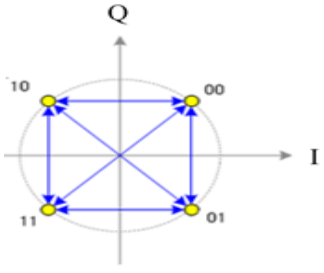

Fig. 7. – QPSK signal constellation

D. Error Vector Magnitude

EVM, also called the Recieved Consellation Error (RCE), is a measure used to quantify the performance of the transmitter or receiver in wireless digital communication. A signal sent by an ideal transmitter or received by an ideal receiver would have all the constellation points precisely in the ideal locations, however due to several imperfections in the implementation (carrier losses, low image rejection rate, presence of phase noise) The constellation points deviate from the ideal places. In other words, it allows measuring how far the actual (measured) points are, from the ideal locations [10].

EVM is therefore an essential parameter for modulation accuracy, since it is a way of measuring and evaluating multi-level and multiphase modulation methods, such as M-QAM and M-PSK [13]. The discrepancy between the vectors of real and ideal symbols is quantified through an error vector, as shown in Figure 8.

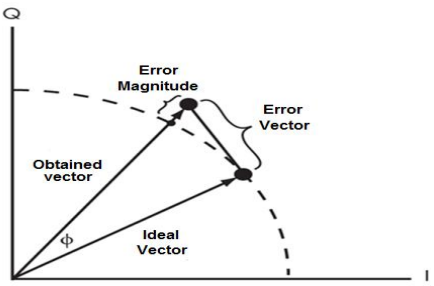

Fig. 8. – EVM

EVM is, therefore, the relation between the power of the error vector and the power of the reference vector, related to the ideal constellation. The EVM can be defined in decibels (dB) or percentage (%) as follows:

$$EVM(\text{dB}) = 10log_{10}\left(\frac{P_{erro}}{P_{ref}}\right) \quad (10)$$

$$\text{EVM}(\%) = \sqrt{\frac{P_{error}}{P_{ref}}} \times 100 \quad (11)$$

where Perror and Pref are the mean square power (RMS) of the error vector and the mean point (mean power) in the reference signal constellation; Iref and Qref are the ideal phase and quadrature signals; Ik and Qk are the signals transmitted in phase and in quadrature [10]. The EVM can also be represented as follows:

$$\text{EVM (RMS)} = \frac{1}{N} \times \sum_{K=1}^{N} \sqrt{\frac{(I_k - I_{ref})^2 + (Q_k - Q_{ref})^2}{(I_{ref} + Q_{ref})^2}} \quad (12)$$

where N is the number of unique symbols in the constellation.

One example of the EVM quantification is the transmission of a signal in which Gaussian white noise has been added. According to the graphic in Figure 9, the lower the signal-to-noise ratio, the higher the EVM (%). And the higher the signal-to-noise ratio the EVM tends to decrease and stabilize by about 1%, corresponding this value to a system detection limit. Therefore, for values obtained close to 1% (green line), they are not totally accurate.

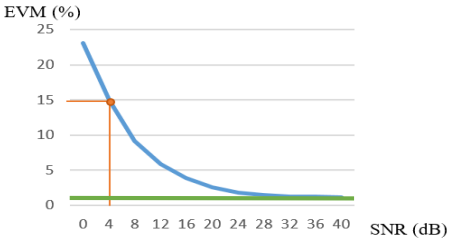

Fig. 9. – EVM/SNR graphic.

Figure 33 shows the QPSK constellation diagram with 1000 symbols, wherein the noise signal ratio is 4 dB. In this case the points that constellation, although concentrating around the ideal points, are quite scattered, possessing an EVM of 15%. A value of this magnitude is sufficient to cause errors in the transmission, in which case it originated the transmission of two wrong bits.

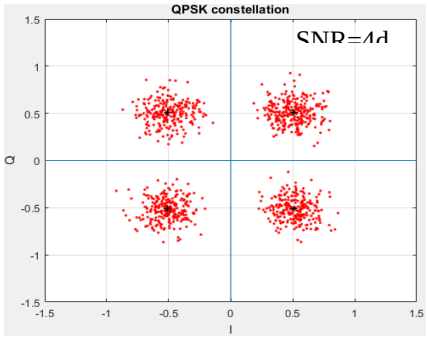

Fig. 10. – EVM/SNR graphic; QPSK constellation with SNR=4dB

In the connection to be made, it will be necessary to use an attenuator filter, given the high power of the laser. This being the only attenuating factor considered in the connection, so that there will be no atmospheric losses during the connection and, as such, the obtained EVM is expected to be close to the detection limit value, that is, close to 1%.

III. Hardware and Software Resources

For the development of the optical module an analog device called ADALM1000 was used. The device has two analog channels (A and B), each capable of generating and measuring analog signals with a maximum sampling rate of 100 kHz. Being powered directly by USB, it supports the OS X, Windows and Linux operating systems [14]. Figure 11 shows a photograph of the ADALM1000 board and its ports of entry.

As an operating system, it was proposed to use Windows and the tests are performed using MATLAB software (v2016a).

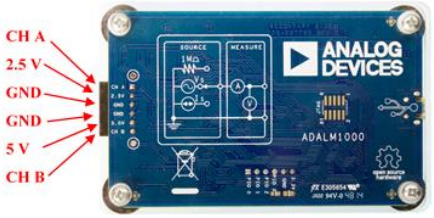

Fig. 11 – ADALM1000

IV. BPSK IMPLEMENTATION

As first implementation phase of the optical module, an LED is defined as an optical emitter. The format used in this system is Binary Phase Shift Keying. In this sense and as shown in Figure 12, an electric subcarrier is used to modulate the optical carrier generated by the optical emitter so that it can be directly modulated and the emitted signal being directly detected by a photodetector, which will be placed at the front, with a minimum distance of 5 mm. For this, channel B has been defined as the output channel, which will feed the LED and channel A as the input channel, which will receive the signal captured by the photodetector. Between channel B and LED, it was necessary to place a resistor in series to limit the maximum current output. For this purpose, a resistance of 270 Ω was used.

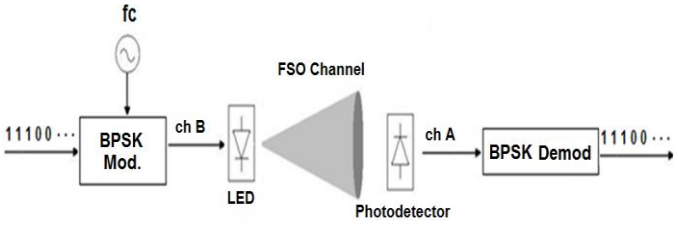

Fig. 12 – BPSK configuration system

The used LED is designated by IF-E96 and is manufactured by Industrial Fiber Optics, Inc. It allows reasonable rhythms of transmission (5 Mps) and emits in the visible spectral region, of red colour, with 660 nm [15]. The photodetector used for signal reception is designated by DET10/AM, of silicon (Si), is manufactured by Thorlabs and is designed to detect optical signals between 200 nm and 1100 nm [16].

A. Transmission window

Before carrying out the transmission of the optical system, it is necessary to study the behavior of the LED. In Figure 13, the x axis represents the voltage introduced into the LED. The y axis represents the voltage read by the photodetector during the process, which corresponds to the optical power emitted by the LED. As can be seen, the photodiode does not read values below approximately 1.8 V, due to the fact that the LED only operates with polarization voltages higher than this value. As such, it has been defined that the most appropriate range to transmit the signal is from 3 to 5 V, where the LED shows a more linear curve.

Fig. 13 – Optical power emitted by the LED as a function of the bias voltage

B. Transmission

A sine wave with a sampling frequency of 1000 Hz and a subcarrier frequency of 50 Hz was considered, and a random sequence of 10 bits was defined to be transmitted. This means each cycle will have 20 samples and each bit will correspond to 5 cycles, that is, 100 samples. Therefore, knowing that the device has capacity to perform 100000 samples per second, the transmission rate will be 1kbit/s. In Figure 14, in red is the representation of the digital signal to be transmitted with the randomly generated sequence "1110011001", and the subcarrier S(t) is shown in blue. It should be noted that the digital signal was encoded in NRZ format.

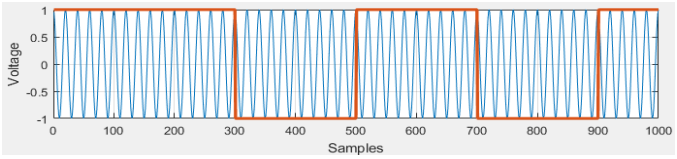

Fig. 14 – Digital Signal (red); Subcarrier (blue)

Then, in order to perform the modulation, the digital signal will control the phase of the carrier. Note that when a bit change occurs, a 180 ° transition also occurs. The subcarrier then modulates the LED in amplitude, which in turn emits the signal through channel B. As a result of this operation, a modulated optical signal Sbpsk(t), shown in Figure 15, is obtained.

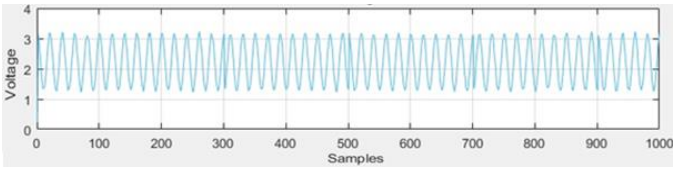

Fig. 15 – Obtained BPSK modulated signal

C. Reception

After the modulated optical carrier emission, it is subsequently captured by the photodetector, in channel A, through direct detection. In order to extract the electric carrier from the optical signal, the received signal Sbpsk(t) was first multiplied again by the carrier wave S(t), obtaining the represented wave of Figure 16. As can be seen, in situations where the bit is 1, the modulated component is mostly above the zero level, while when the bit is 0, the modulated component is mostly below the zero level. It is expected that the wave is not equal to that of the previous chapter, due to the processing performed by the photodetector, namely in the slight increase in signal amplitude.

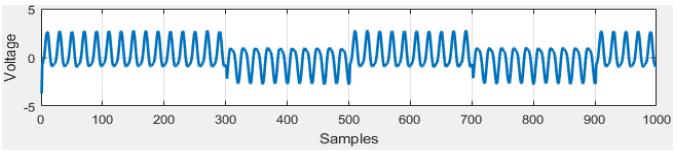

Fig. 16 – Signal obtained, after multiplication.

In order to remove the oscillatory component, a buterworth low-pass filter was used. This filter is developed so as to obtain a frequency response as flat as mathematically possible. In this way, it was possible to determine the original baseband signal and hence the original bit stream. It is noted in Figure 17 that the signal amplitude decreases by half, as a consequence of the application of the filter. It is also important to note that the higher the filter order and the lower the filter cutoff frequency, the longer the signal delay in the transitions. This explains why the recovered signal is not perfect and still contains residual oscillatory component.

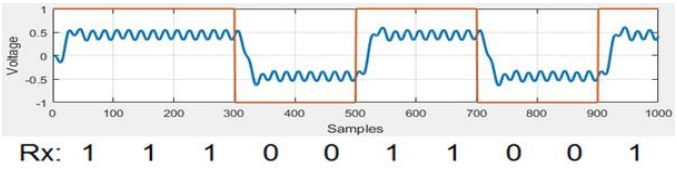

Fig. 17 – Original signal obtained (blue), after filtration.

In Figure 18, the signal constellation is shown. The method used to determine it, required the integration of 10 core samples for each bit. The calculated value of each corresponds to its respective symbol. Although the values are not all the same, it is not particularly important where the points are positioned.

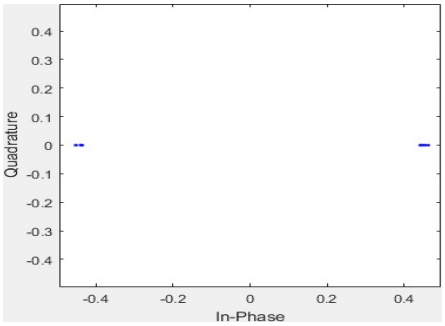

Fig. 18 – Obtained constellation.

V. QPSK IMPLEMENTATION

In the previous chapter we described the implementation of the optical communication module with the BPSK format, in which an LED was used as the optical emitter. It was verified that this module performs well, demonstrating that the concept is feasible. In order to achieve the objectives initially defined, the previously implemented module will be adapted to be able to use the QPSK multilevel format and as optical emitter a semiconductor laser. In this way, it will be possible to measure the EVM and consequently quantify the system performance.

The configuration of the system is maintained, with channel B being defined as the output channel, which will feed the semiconductor laser, and channel A as the input channel, which will receive the signal captured by the photodetector. The photodetector used was the same, the DET10A/M]. In this case, it will be positioned 20 cm in front of the optical emitter. The laser used is designated MRL-III-635 and is manufactured by Changehun New Industries Optoelectronics Tech, Co, Ltd. It has a red diode with a wavelength of 635 nm and is characterized by having a very long lifetime, low cost and is easy to operate. It has a considerable power output of 300 mW [17]. Due to the fact that the laser power is too high, a filter station was placed between the connection, in order to attenuate the output power.

The filter station used was a FW1AND, made by Thorlabs, and the chosen attenuator filter has an optical density of 3. According to the values presented by Thorlabs, for an optical density 3 and a wavelength of 635 nm, the transmission value is only 0.1035% [18]. This value corresponds to an attenuation of 29.85 dB and, therefore, it is considered that up to this value, the use of the laser is feasible. Figure 19 shows the attenuation values obtained from equations (1) and (2), with five different weather conditions, for a wavelength of 635nm. For each weather condition, a range of visibility was also defined [8]:

Weather Condition	Clear	Haze	Thin Fog	Light Fog	Heavy Fog
Visibility (km)	20	2	1.5	1	0.5
Attenuation (dB/km)	0.72	8.22	10.64	16.14	34.7

Fig. 19 – Atmospheric attenuation in (dB/km) as a function of visibility at 635 nm.

According to the values obtained in the table, the laser achieves all climatic conditions reaches, except in situations of heavy fog, where the attenuation is higher than the defined experimental value (29.85 dB). However, it is important to note that the beam divergence and the received power in the optical receiver are still to be considered, since only then is it possible to correctly analyze the laser range, for different situations.

A. Transmission

It was initially defined that each cycle consists of 10 samples since it was the minimum value tested that best suits to correctly define a sinusoidal wave, reason why, if it were inferior, the signal would resemble a triangular wave. Each bit theoretically corresponds to four cycles and, as such, to 40 samples. However, since it is a QPSK modulation, in practice, it is possible to double the transmitted information and as such, each bit corresponds to 20 samples. Since the analog device can read 100000 samples per second, the tested signal then has a frequency of 10 kHz and the transmission rate is 5 kbit/s, or 2500 symbols per second.

As a way to measure the EVM and thus evaluate the system performance, a signal transmission (S1) with 40,000 samples is tested. This means that 2000 bits will be transmitted and the constellation diagram will have 1000 symbols. The parameter to be quantified is the EVM (RMS), in percentage.

The Figure 20a represents the first 200 samples of the in-phase component of signal S1, Figure 20b represents the first 200 samples of the quadrature component.

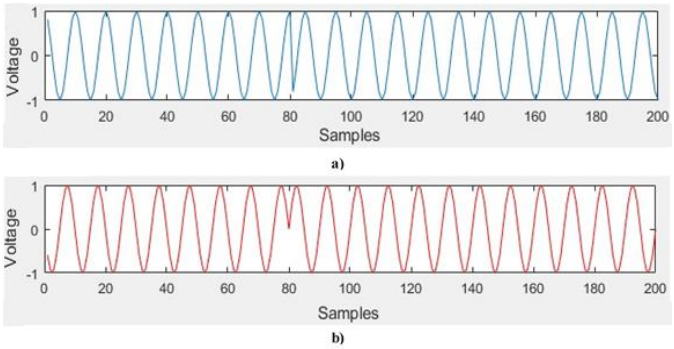

Fig. 20 – A) S1 phase component; B) S1 quadrature component.

After multiplication of the two components, the signal S1 is then obtained, as the first 200 samples being presented in Figure 21.

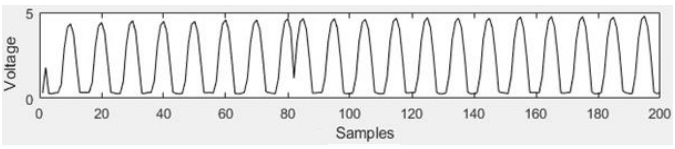

Fig. 21 – A) QPSK modulated signal

B. Reception

After the signal S1 is sent by channel B and received by channel A, the original signal is recovered. First, the signal received was multiplied by in phase Ci (t) and quadrature Cq (t) carrier waves. Figure 22 represents the first 200 samples of each. Note that there is some lag in the signal amplitude. However, it is possible to verify that the amplitudes are changed according to the amplitude of the digital signal.

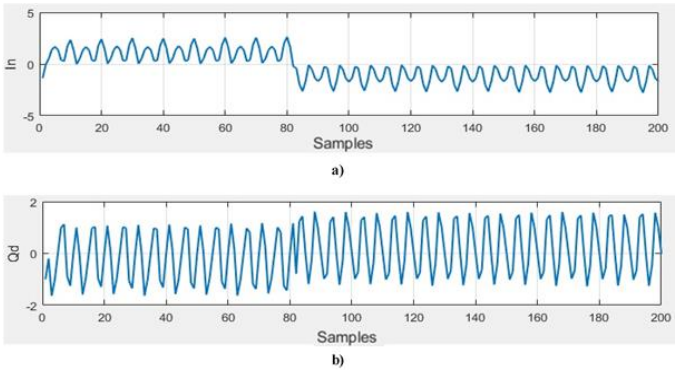

Fig. 22 – A) S1 in-phase component; B) S1 quadrature component.

After multiplication, the oscillatory component was removed with the application of the butterworth low-pass filter. In this way, it was possible to determine the original baseband signal in-phase and quadrature and consequently the original bit sequence. The recovered signal is still not perfect and still contains residual oscillatory component and excessive amplitude, which can lead to amplitude and phase imbalances in the signal constellation. This is essentially due to the fact that semiconductor lasers are inherently non-linear, which makes analogue transmissions more difficult. They are also very sensitive to temperature and current fluctuations, which can cause variations in the wavelength produced. Figure 23 represents the first 200 samples of each component.

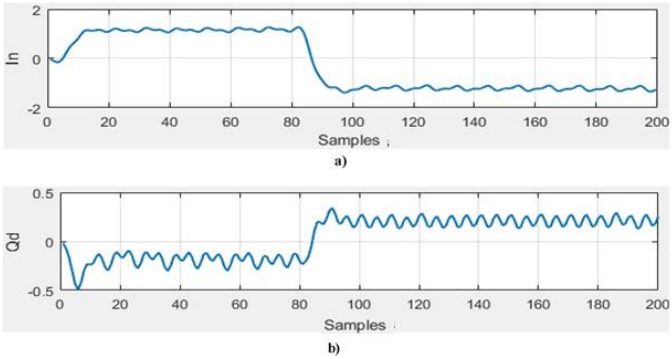

Fig. 23 – Digital recovered components.

In Figure 24, is shown the constellation of S1 signal obtained from the previously recovered signal. The method used is the same as in the BPSK, that is, analytically by integrating the 10 core samples of each bit, the values calculated from the first signal correspond to the real component and the values calculated from the second signal correspond to the imaginary component constellation points. As you can see, the points obtained (red) are quite out of phase from the ideal points (black), and as such, it is necessary to turn some degrees.

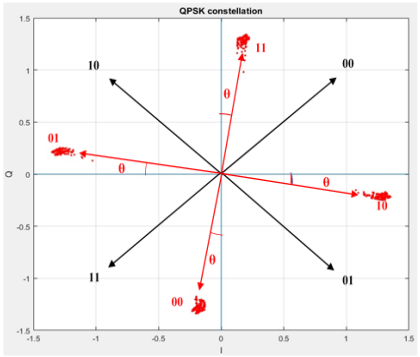

Fig. 24 – A) S1 phase component; B) S1 quadrature component.

From the angle θ obtained, it will be possible to determine the degrees of compensation Δθ. Given that θ = 8º, then:

$$\Delta\theta = \theta + 45º + 90º = 8º + 135º = 143º$$

In order to compensate the constellation points, it is necessary to rotate 143 degrees, so that the points (in red) are as close as possible to the ideal points (in black). Figure 5 shows the resulting diagram. Regarding the magnitude of the signal, it remains approximately equal:

$$k = 250 \rightarrow \begin{cases} P_{250} = 0.2433 + 1.3172 * i \\ P'_{250} = -0.987 - 0.9055 * i \end{cases} \Leftrightarrow \begin{cases} |P_{250}| = 1.3397 \\ |P'_{250}| = 1.3394 \end{cases}$$

where P_{250} is the 250th constellation point of S_1 signal and P_{250}' corresponds to the compensated point of P_{250}.

Figure 25 shows the diagram obtained after this operation. In spite of presenting the points with some imbalance, they are much closer to each other when compared to the diagram in Figure 9b, where a 4dB Gaussian white noise was applied and as such it is expected that the EVM is much smaller in the results obtained.

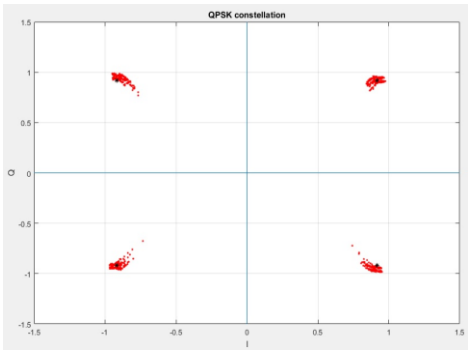

Fig. 25 – S1 Constellation diagram, after compensation

After obtaining the compensated constellation diagram, the signal S1 EVM(%) is calculated. Applying the formula 12, the following EVM was obtained in percentage:

Signal	S_1
EVM (%)	1,3041

Fig. 26 – Table showing the EVM obtained for S1 signal.

As can be seen, for a signal with 1000 symbols, that is, 2000 bits, the EVM is 1.3041%. This optimum value is essentially due to the absence of noise and losses and also due

to the implementation method used throughout the process. However, it is important to note that this value is not totally accurate, due to the detection limit being close to 1%.

Throughout the processing, the module took approximately 37 minutes to be transmitted, being 5550 times higher than the predicted theoretical value of 0.4 seconds. This implies that the processing and the algorithm need to be optimized.

Even so, the system is adequate to the objectives previously established for the dissertation, since it allows modulation of the subcarrier and receive the correct bit sequence taking into account the low value of the EVM, thus being able to constitute a solid base for the development and implementation of a backhaul system.

VI. Conclusions

As a core element in this dissertation, a low-cost optical communications module was developed and implemented in the visible spectral region and is based on the direct modulation of the optical emitter. In a first approach, which was intended to prove the concept of modulation of the subcarrier, it was decided to use a LED as an optical emitter and the BPSK modulation format.

Regarding the low-pass filter application, it still requires better optimization, because the recovery of the baseband signal is far from perfect. However, by analysing the obtained results, one can conclude that the concept was successfully proven by which the sequence of bits was transmitted successfully. In a second approach, it was intended to quantify the performance of the system by measuring the EVM from the constellation diagram. For this, we chose a semiconductor laser as the optical emitter and the QPSK modulation format. From the transmission of a signal with 1000 symbols, an EVM of 1.3041% was obtained, which is a very promising result, revealing the high potential of this communication module. Regarding the transmission time, taking into account that the sampling rate is 100 kHz and the signal has 40000 samples, the expected transmission time would be 0.40 seconds. However, due to the signal processing performed by MATLAB and the hardware, the transmission took 37 minutes, 5550 times higher than the predicted theoretical value. This implies that in terms of processing, the algorithm used needs some optimization.

With regard to the analogue device used, ADALM1000 proved to be a very useful tool and simple to manipulate, with respect to the reading and sending of signals. Although its frequency cannot be manipulated, remaining at 100 kHz, it was fit to be of use to the previously established objectives for the dissertation, because it allowed modulation of the subcarrier and the reception of the correct bit sequence, thus being able to constitute a solid base for the development and implementation of a backhaul system.

References

I would like to thank Instituto Superior Técnico for the valuable contribution for the aggrandizement of my academic career, especially to Professor Paulo André, for the tireless and effective way in which he gave his guidance and valuable help in the development of this work

References

[1] Henniger, H., & Wilfert, O., "An Introduction to Free-space Optical Communications", vol. 19, no. 2, pp. 203–212, 2010.

[2] Kaushal, H., Kaddoum, G., & Engineering, C., "Free Space Optical Communication : Challenges and Mitigation Techniques", pp. 1–28.

[3] Gupta , A. & Jha, R., "A Survey of 5G Network: Architecture and Emerging Technologies", vol. 2, 2015

[4] MRV TereScope, "TereScope 10GE" [Online]. Available: https://web.archive.org/web/20140818135956/http://www.jazdcommunications.com/commtech/company/MRV/TereScope-10GE.htm?supplierId=50004089&productId=5006 0878 [Accessed: 15-Nov-2016].

[5] Artolink, "10 Gps Through The Air" [Online]. Available: http:// artolink.com/ page/free_ space_optics_Artolink_news/#new10g. [Accessed: 17-Nov-2016]

[6] Alkholidi, A. G. (2014). Free Space Optical Communications: Theory and Practices.

[7] Tang, X., "Polarisation Shift Keying Modulated Free-Space Optical Communication Systems", Dissertation presented in partial fulfillment of the requirements of the University of Northumbria, in Newcastle, for Doctor degree, 2012.

[8] Ali, M. & Mohammed, M., "Effect of Atmospheric Attenuation on Laser Communications for Visible and Infrared Wavelenghts", vol. 16, no. 3, pp. 133-140, 2013.

[9] N. Vlajic, "Analog Transmssion of Digital Data: ASK, FSK, PSK, QAM", Material de apoio à unidade curricular "Signal Processing and Linear Systems II", Universidade de Stanford, San Francisco, EUA, 2016.

[10] AVNET Reach Further, "Understanding Quadrature Phase Shift Keying", [Online] Available: https://www.allaboutcircuits.com/ technical-articles/quadrature-phase-shift-keying-qpsk- modulation/ [Acessed: 19-FEV-2017].

[11] Wikipédia, "Conceptual transmitter structure for QPSK", [Online] Available: https://en.wikipedia.org/wiki/ Phase-shift_keying#/media/File:Transmisor_ QPSK_2.png [Acessed: 17-JFEV-2017.

[12] Wikipédia, "Reciever structure for QPSK", [Online] Available: https://en.wikipedia.org/wiki/ Phase-shift_keying#/media/File:Receiver_ QPSK_2.png [Acessed: 19-JFEV-2017.

[13] Mohammadi, A. & Ghannouchi, F., *RF Transceiver Design for MIMO Wireless Communications*, Springer, 2012.

[14] Analog Devices, "ADALM1000 Overview", [Online] Available: https://wiki.analog.com/ university/tools/m1k [Acessed: 15-NOV-2016].

[15] Industrial Fiber Opics, Inc, "Plastic Fiber Optic Red LED", *Prod. Data*, 2006.

[16] Thorlabs, "DET10A/M Si Biased Detector", *User Guide*, 2013.

[17] CNILASER, "MRL-III-635/1-500mW", *Data Sheet*, 2016.

[18] Thorlabs, "Manual Filter Wheel Mounts with Neutral Density Filters", [Online] Available: https://www.thorlabs.com/newgrouppage9.cfm?objectgroup_id =1444&pn=FW1AND#1444.